



THE UNIVERSITY *of* EDINBURGH

Edinburgh Research Explorer

Modulation theory solution for nonlinearly resonant, fifth order Korteweg-de Vries, non-classical, traveling dispersive shock waves

Citation for published version:

Hoefer, MA, Smyth, N & Sprenger, P 2019, 'Modulation theory solution for nonlinearly resonant, fifth order Korteweg-de Vries, non-classical, traveling dispersive shock waves', *Studies in Applied Mathematics*, vol. 142, no. 3, pp. 219-240. <https://doi.org/10.1111/sapm.12246>

Digital Object Identifier (DOI):

[10.1111/sapm.12246](https://doi.org/10.1111/sapm.12246)

Link:

[Link to publication record in Edinburgh Research Explorer](#)

Document Version:

Peer reviewed version

Published In:

Studies in Applied Mathematics

General rights

Copyright for the publications made accessible via the Edinburgh Research Explorer is retained by the author(s) and / or other copyright owners and it is a condition of accessing these publications that users recognise and abide by the legal requirements associated with these rights.

Take down policy

The University of Edinburgh has made every reasonable effort to ensure that Edinburgh Research Explorer content complies with UK legislation. If you believe that the public display of this file breaches copyright please contact openaccess@ed.ac.uk providing details, and we will remove access to the work immediately and investigate your claim.



Modulation theory solution for nonlinearly resonant, fifth order Korteweg-de Vries, non-classical, traveling dispersive shock waves

By Mark A. Hoefer¹, Noel F. Smyth² and Patrick Sprenger¹

A new class of resonant dispersive shock waves were recently identified as solutions of the Kawahara equation— a Korteweg-de Vries (KdV) type nonlinear wave equation with third and fifth order spatial derivatives— in the regime of non-convex, linear dispersion. Linear resonance resulting from the third and fifth order terms in the Kawahara equation was identified as the key ingredient for non-classical dispersive shock wave solutions. Here, nonlinear wave (Whitham) modulation theory is used to construct approximate non-classical traveling dispersive shock wave (TDSW) solutions of the fifth order KdV equation without the third derivative term, hence without any linear resonance. A self-similar, simple wave modulation solution of the fifth order, weakly nonlinear KdV-Whitham equations is obtained that matches a constant to a heteroclinic traveling wave via a partial dispersive shock wave so that the TDSW is interpreted as a nonlinear resonance. The modulation solution is compared with full numerical solutions, exhibiting excellent agreement. The TDSW is shown to be modulationally stable in the presence of sufficiently small third order dispersion. The Kawahara-Whitham modulation equations transition from hyperbolic to elliptic type for sufficiently large third order dispersion, which provides a possible route for the TDSW to exhibit modulational instability.

Address for correspondence: Department of Applied Mathematics, University of Colorado Boulder, Boulder, Colorado, U.S.A. 80309 email:

1. Introduction

Dispersive shock waves (DSWs), also termed undular bores in geophysical fluids applications, are a nonlinear dispersive wave form with widespread occurrence in many physical media, including fluid mechanics (water wave theory), oceanography, meteorology, optics and condensed matter. Indeed, they are just as widespread in nature as the more commonly known solitary wave or soliton [1]. In geophysics, bores are of two general types: viscous bores, which are steady due to a balance between viscosity and dispersion [1, 2, 3], and undular bores, which are unsteady and continually expand in time due to negligible viscous effects [4]. The present work focuses exclusively on dissipationless undular bores, which we term DSWs throughout.

The classic example of a DSW occurs in coastal regions with strong tidal dynamics and suitable coastal topography to enhance the flow, examples being the Severn Estuary in England, the Bay of Fundy in Canada and the Pororoca tidal bore on the Amazon River in Brazil. DSWs also arise during the generation of waves in a fluid with imposed forcing, such as by a ship or by fluid flow over topography when the imposed flow velocity is near a linear long wave speed for the fluid [5, 6, 7, 8, 9]. An example of the former are waves generated when a ship moves through a fluid whose Froude number is near unity [10]. Similar DSWs generated by flow over topography are morning glory clouds [11, 12, 13] and the internal DSWs generated by the flow of the semi-diurnal internal tide over a shelf-break [14]. DSWs have also been found as solutions of equations that model the buoyant flow of magma through the Earth's mantle [15, 16, 17, 18]. These equations, in fact, coincide with the long wave interfacial equations for the conduit flow of a buoyant, viscous fluid through a miscible, much more viscous fluid [18, 19]. Other DSW application areas include nonlinear optics (photorefractive crystals [20, 21, 22, 23], nonlinear optical fibers [24, 25], nonlinear thermal optical media [26, 27], and colloidal media [28, 29]) and Bose-Einstein condensates [30, 31] and thin-film magnetic materials [32].

Mathematically, a DSW can be understood as an unsteady, modulated wavetrain that consists of two distinguished limits: the zero wavenumber, solitary wave limit and the zero amplitude, linear dispersive wave limit. Both limits allow for a smooth transition of the oscillatory DSW to non-oscillatory states and are the key features com-

mon to DSWs [4]. The DSW orientation—the location of the solitary wave edge relative to the linear wave edge—is typically determined by the sign of the governing equation’s linear dispersion relation curvature. The solitary wave edge polarity, positive (wave of elevation) or negative (wave of depression), is determined by the combined effects of the nonlinear hydrodynamic flux curvature and linear dispersion curvature [33].

Until recently, most DSW research has focused on convex media, i.e., nonlinear wave equations whose nonlinear hydrodynamic flux and linear dispersion relation have no inflection points. We refer to DSWs in convex media as classical in the sense that they generically resemble the canonical DSW first constructed by Gurevich and Pitaevskii for the Korteweg-de Vries (KdV) equation [34]. DSWs in the presence of nonconvex flux, however, can exhibit non-classical structure, such as in the undercompressive DSW and the contact DSW [33]. For non-convex linear dispersion, non-classical DSW behavior can also emerge. In the absence of resonance, non-convex linear dispersion can give rise to modulational instability in the vicinity of the DSW’s linear wave edge, originally termed DSW implosion [18]. In the recent work [35], non-convex linear dispersion that coincides with a linear resonance between a DSW and small amplitude, linear dispersive waves was shown to give rise to new DSW types in the Kawahara equation [36]

$$\frac{\partial u}{\partial t} + 6u \frac{\partial u}{\partial x} + \epsilon \frac{\partial^3 u}{\partial x^3} + \frac{\partial^5 u}{\partial x^5} = 0. \quad (1)$$

Here, $\epsilon > 0$ is a parameter that signifies the strength of third order dispersion relative to fifth order dispersion. The linear dispersion relation for the Kawahara equation (1) on the constant or slowly varying background \bar{u} is

$$\omega(k) = 6\bar{u}k - \epsilon k^3 + k^5, \quad (2)$$

which is non-convex when $\epsilon > 0$. In this case, there exist elevation solitary wave solutions of equation (1) whose phase velocity coincides with the phase velocity of linear waves, leading to resonance and the decay of the solitary wave [37, 38, 39]. Note that for $\epsilon < 0$ no resonance occurs as depression solitary wave solutions have negative phase velocity, whereas linear waves have only positive phase velocity.

An analysis of resonant, non-classical DSWs governed by the Kawahara equation (1) has been presented in [35], which identified three dis-

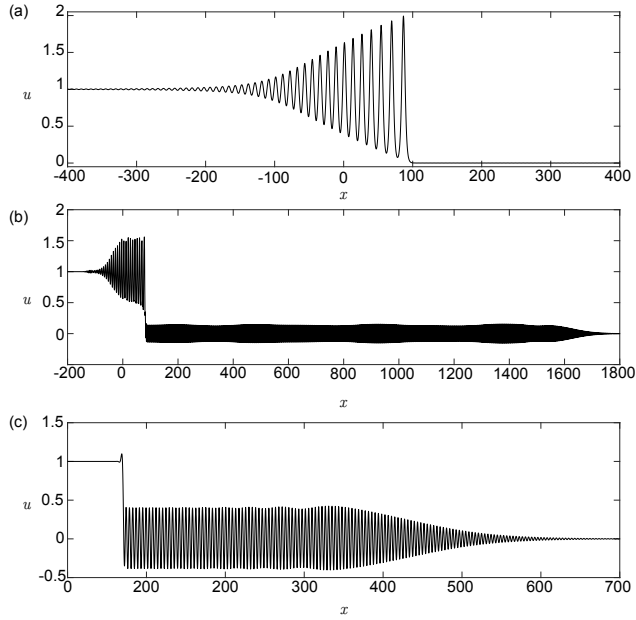


Figure 1. Non-classical dispersive shock wave types arising from a unit jump initial condition (3), $u_- = 1$, $u_+ = 0$, for the Kawahara equation (1). Initial condition: red (dashed) curve; solution at $t = 30$: black (solid) curve. (a) resonant DSW (RDSW), a perturbed KdV DSW with exponentially small radiation from the solitary wave, $\epsilon = 8$. (b) crossover DSW where the radiation amplitude is large and there are wave modulations throughout the structure, $\epsilon = 5$. (c) traveling DSW (TDSW), from left, a partial, non-monotonic solitary wave rapidly transitions to non-linear periodic traveling wave that is modulated to the constant $u_+ = 0$, $\epsilon = 1$.

tinct dynamical regimes as a function of the initial jump height for fixed ϵ . By appropriate rescaling of dependent and independent variables, we can restate these results for equation (1) in terms of variable ϵ with a fixed initial jump height $u_- - u_+$, where

$$u(x, 0) = \begin{cases} u_-, & x < 0 \\ u_+, & x > 0 \end{cases} . \quad (3)$$

To simplify calculations here we will typically take $u_- = 1$ and $u_+ = 0$. For large, positive ϵ , the long-time dynamics of the Kawahara equation (1) subject to the initial data (3) consist of a perturbed KdV DSW accompanied by a small resonant wavetrain (Figure 1(a)). For moderate ϵ , a crossover DSW regime was identified for which the resonant wavetrain's amplitude is significant and has a major effect on the dynamics (Figure 1(b)). The final type, for small, positive ϵ , was termed a traveling DSW (TDSW) because its trailing portion consists of a genuine traveling wave solution of the Kawahara equation (1) (Figure 1(c)). This traveling wave is an equilibrium heteroclinic to a periodic orbit and was identified with a nonlinear resonance because it resembles a partial, non-monotonic solitary wave solution of the Kawahara equation (1) moving with the same speed as a nonlinear periodic traveling wave. Aside from its leftmost solitary wave edge and rightmost linear wave edge, the TDSW has little qualitative resemblance to a classical DSW.

The analysis of the TDSW undertaken in [35] was based on the construction of an approximate traveling wave solution for $\epsilon > 0$. This approximate solution does not describe the full TDSW structure because the nonlinear, resonant wavetrain eventually decays to the constant, far field value u_+ , as shown in Fig. 1(c). Moreover, because ϵ in the Kawahara equation (1) was fixed and the jump height was varied, the TDSW was shown to exist only above a jump threshold.

In this paper, we construct approximate TDSW solutions of the fifth order KdV equation (KdV5)

$$\frac{\partial u}{\partial t} + 6u \frac{\partial u}{\partial x} + \frac{\partial^5 u}{\partial x^5} = 0, \quad (4)$$

subject to the initial data (3). We obtain solutions for arbitrary negative jumps $u_- > u_+$ and demonstrate that neither linear resonance nor non-convex dispersion are required for TDSW existence. In this regard, the TDSW can be interpreted as a nonlinear resonance between a solitary wave on the left and a nonlinear periodic wave on the right with

coinciding phase speeds. We derive the Whitham modulation equations for the KdV5 equation (4) in the weakly nonlinear regime and identify a self-similar, simple wave solution that, along with a heteroclinic solution, yield a complete, self-consistent construction of the entire TDSW structure that is missing from [35]. In addition, we derive the Whitham modulation equations for the Kawahara equation with $\epsilon > 0$ and demonstrate their hyperbolicity, hence modulational stability of the TDSW, for sufficiently small ϵ . We also demonstrate that the Kawahara-Whitham equations are elliptic in certain parameter regimes. These results suggest a possible route for the TDSW to transition to the crossover regime for sufficiently large ϵ via modulational instability. We also provide further analysis of the crossover regime, concluding that all the waves contained in the DSW resonate, as opposed to just the solitary wave, as was assumed in previous studies [40, 41, 42, 43].

Another context in which linear resonance and DSWs have been studied is the defocusing nonlinear Schrödinger (NLS) equation when higher order dispersion is included [40, 41, 42, 43]. Resonant DSWs have also been found to occur for the equations governing nonlinear optical beam propagation in nematic liquid crystals in the defocusing regime [44, 45], described by an extended NLS equation. In both cases, for sufficiently small hydrodynamic transitions, these NLS-type equations can be asymptotically reduced to the much simpler unidirectional, scalar Kawahara equation [35, 45] or the KdV5 equation (4) at criticality ($\epsilon = 0$). Under appropriate degeneracy conditions, any Eulerian dispersive hydrodynamic system of equations can be reduced to the Kawahara equation, e.g., shallow water waves with strong surface tension [35] and internal water waves under an ice sheet, for which elasticity is coupled to water wave motion [46]. It has been shown that, under certain conditions, the Kawahara equation arises generically for slow modulations of a periodic wavetrain [47]. Consequently, the results of the present work apply to resonant DSWs in other physical media as well.

2. KdV5-Whitham modulation equations in the weakly nonlinear limit

One approach to describing DSWs is Whitham's averaging principle [49, 48, 1], which treats the DSW as a slowly varying modulation of a family of exact periodic, traveling wave solutions to the governing partial

differential equation (PDE). When the resulting modulation equations are hyperbolic, the wavetrain is modulationally stable [1, 54]. We now obtain the KdV5-Whitham equations in the weakly nonlinear regime.

The KdV5 equation (4) possesses a Lagrangian formulation when expressed in terms of the potential ϕ with

$$u = \frac{\partial \phi}{\partial x}. \quad (5)$$

The Lagrangian density is

$$L = \frac{1}{2} \phi_t \phi_x + \phi_x^3 + \frac{1}{2} \phi_{xxx}^2, \quad (6)$$

so that critical points of the Lagrangian $\int L \, dx dt$ satisfy $(L_{\phi_t})_t + (L_{\phi_x})_x + (L_{\phi_{xxx}})_{xxx} = 0$, which is equivalent to the KdV5 equation (4). The Whitham modulation equations are obtained by integrating the Lagrangian density (6) over a family of periodic traveling waves and taking variations with respect to the periodic wave parameters, thus yielding a closed system of equations that describe a modulated periodic wave [1, 48, 49], though we are not aware of explicit traveling wave solutions to (4). Here, we consider the weakly nonlinear limit of the KdV5-Whitham equations by approximating the periodic traveling wave solution of equation (4) with amplitude a , mean \bar{u} and phase $\theta = kx - \omega t$ by the Stokes expansion

$$u = \bar{u} + a \cos \theta + \alpha_2 a^2 \cos 2\theta + \dots, \quad 0 < a \ll 1. \quad (7)$$

Without loss of generality, we have chosen the solution to be 2π periodic in θ . For modulation theory, any period that is independent of the wave parameters will do. We also expand the frequency in powers of the small parameter a and substitute the expansion of u and ω into KdV5 (4). Equating like powers of a and eliminating secular terms, the amplitude correction is

$$\alpha_2 = -\frac{1}{10k^4} \quad (8)$$

and the nonlinear dispersion relation is

$$\omega = 6\bar{u}k + \omega_0 + \omega_2 a^2, \quad \omega_0 = k^5, \quad \omega_2 = -\frac{3}{10k^3}. \quad (9)$$

The Stokes expansion (7) can be used to find modulation equations for KdV5 (4). This derivation of the modulation equations for the fifth

order KdV equation is similar to that for the KdV equation [1, 49]. We then seek a slowly varying Stokes wave

$$\phi = \psi + \Phi(\theta), \quad (10)$$

with the following wavetrain parameters— amplitude a , wavenumber k , frequency ω and mean height \bar{u} — functions of x and t , slowly varying with respect to θ . The modulation wavenumber and frequency are defined in terms of the phase θ by $k = \theta_x$ and $\omega = -\theta_t$. The function Φ has zero period-mean and the function ψ accounts for the mean of the varying wavetrain, given by $\bar{u} = \psi_x$. We also set $\gamma = -\psi_t$. Substituting the modulation wavetrain (10) into the Lagrangian density (6) gives

$$L = \frac{1}{2} \left[-\gamma + \frac{\omega}{k} \bar{u} \right] u - \frac{1}{2} \frac{\omega}{k} u^2 + u^3 + \frac{k^4}{2} u_{\theta\theta}^2, \quad (11)$$

using $u = \phi_x = \bar{u} + k\Phi_\theta$. The averaged Lagrangian is now obtained by substituting the Stokes expansion (7) into the Lagrangian (11) and averaging by integrating over a wave period [1]. This results in the averaged Lagrangian

$$\begin{aligned} \mathcal{L} = & -\frac{1}{2} \gamma \bar{u} + \bar{u}^3 + \left(\frac{3}{2} \bar{u} - \frac{1}{4} \frac{\omega}{k} + \frac{1}{4} k^4 \right) a^2 \\ & - \frac{1}{200k^4} \left[\frac{\omega}{2k^5} - \frac{3}{k^4} \bar{u} + 7 \right] a^4 + \mathcal{O}(a^6). \end{aligned} \quad (12)$$

The modulation equations for the slowly varying parameters of the Stokes wave are now obtained by taking variations of this averaged Lagrangian with respect to the phase θ , the mean phase ψ and the amplitude a . For simplicity, we only retain up to $O(a^2)$ terms in the variations. Amplitude variation, $\mathcal{L}_a = 0$, yields the linear dispersion relation $\omega = 6\bar{u}k + k^5$. Mean phase variation $-(\mathcal{L}_\gamma)_t + (\mathcal{L}_{\bar{u}})_x = 0$ determines the mean flow modulation

$$\frac{\partial \bar{u}}{\partial t} + \frac{\partial}{\partial x} \left[3\bar{u}^2 + \frac{3}{2} a^2 \right] = 0. \quad (13)$$

Phase variation $-(\mathcal{L}_\omega)_t + (\mathcal{L}_k)_x = 0$ leads to the conservation of wave action

$$\frac{\partial}{\partial t} \left[\frac{a^2}{k} \right] + \frac{\partial}{\partial x} \left[6\bar{u} \frac{a^2}{k} + 5k^3 a^2 \right] = 0. \quad (14)$$

This modulation system is closed by the conservation of waves $\theta_{tx} = \theta_{xt}$

$$\frac{\partial k}{\partial t} + \frac{\partial}{\partial x} \left[6\bar{u}k + k^5 - \frac{3}{10} \frac{a^2}{k^3} \right] = 0. \quad (15)$$

The weakly nonlinear modulation equations (13)–(15) are valid to order a^2 .

These modulation equations form a hyperbolic system— weakly nonlinear periodic waves are modulationally stable— and can be set in the Riemann invariant form

$$\begin{aligned} \bar{u} - \frac{3}{10} k^{-4} a^2 = R_{\bar{u}} \text{ on } P : \lambda_P = \frac{dx}{dt} = 6\bar{u} + \frac{18}{5} k^{-4} a^2, \quad (16) \\ \frac{24}{\sqrt{30}} \bar{u} + \frac{5}{\sqrt{30}} k^4 - 2a = R_- \text{ on } Q : \lambda_Q = \frac{dx}{dt} = 6\bar{u} + 5k^4 - \sqrt{30}a, \end{aligned} \quad (17)$$

$$\frac{24}{\sqrt{30}} \bar{u} + \frac{5}{\sqrt{30}} k^4 + 2a = R_+ \text{ on } R : \lambda_R = \frac{dx}{dt} = 6\bar{u} + 5k^4 + \sqrt{30}a. \quad (18)$$

Here $R_{\bar{u}}$, R_- and R_+ are constant on their respective characteristics P , Q , and R . We note the ordering of the characteristic velocities $\lambda_P < \lambda_Q \leq \lambda_R$ for $a \geq 0$ and $k > 0$. To compute the approximate Riemann invariants (16)–(18), we expand both the characteristic velocities and Riemann invariants as an amplitude expansion with $0 < a \ll 1$ and retain the first nontrivial order of a . Higher order terms can be computed by retaining more terms in the asymptotic approximation, as well as the Stokes wave expansion. The TDSW for KdV5 will now be studied using the approximate KdV5-Whitham modulation equations (13)–(15).

3. Traveling DSW modulation solution

We now consider DSW evolution governed by the KdV5 equation (4) subject to the step initial data (3). For $u_- < u_+$, the dynamics correspond to a dispersive regularization of a classical rarefaction wave solution for the dispersionless equation $u_t + 6uu_x = 0$. We are interested in the compressive case $u_- > u_+$, which leads to wave breaking and DSW generation. By the scaling and Galilean symmetries of KdV5, we can consider the specific case $u_- = 1$ and $u_+ = 0$, without loss of generality. A numerical simulation for a smoothed initial step is shown in Fig. 2. This solution differs substantially from a classical, KdV DSW

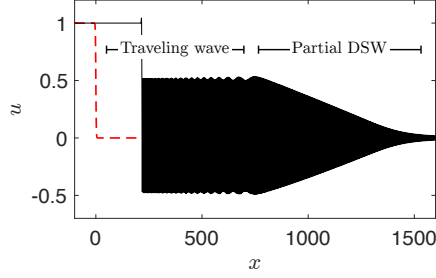


Figure 2. Numerical simulation of the KdV5 equation (4) for smoothed step initial data (3) with $u_- = 1$, $u_+ = 0$. The dashed red curve is the smoothed initial data.

solution with positive dispersion. The leftmost equilibrium, u_- , rapidly transitions to a nearly uniform wavetrain. Ahead of this wavetrain is a modulated wavetrain that gradually transitions to the rightmost level ahead u_+ . What we now show, depicted in Fig. 2, is that the leftmost portion of the TDSW wavetrain is approximately a traveling wave solution to KdV5 and the modulated portion of the TDSW wavetrain is a partial DSW.

Figure 2 is similar to Figure 1(c), the TDSW solution of the Kawahara equation studied in [35]. In that work, the existence, via numerical computation and asymptotics, of a genuine traveling wave solution linking the level behind, u_- , to the periodic nonlinear wavetrain was shown, which agreed with time-dependent evolution of step initial data. Here we demonstrate that the same kind of TDSW dynamics occur for the KdV5 step problem but without the jump threshold required in [35]. Furthermore, we determine the modulation solution corresponding to the partial DSW portion of the TDSW that was missed in [35].

As the partial DSW is traversed upstream from its linear edge—right to left—its increasing amplitude and decreasing wavenumber eventually terminate into the resonant wavetrain as seen in Figure 2. The fact that the partial DSW terminates at an oscillatory wavetrain, rather than a constant level, is the reason it is termed partial. Partial DSWs have been observed in other contexts, such as initial-boundary value problems [9, 50, 51, 52] and initial value problems [53].

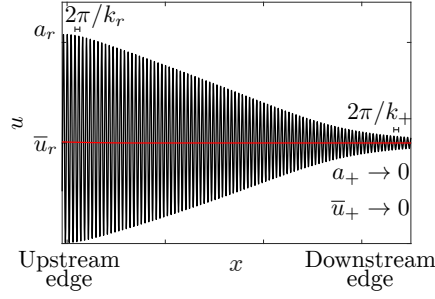


Figure 3. Depiction of leading partial DSW connecting resonant wave-train to leading mean $u = u_+$. The small variation of the mean, \bar{u} is shown in red.

We now use the approximate Riemann invariant form (16)–(18) of the modulation equations to obtain the partial DSW modulation solution. The DSW modulation solution for Riemann problems is often obtained as a self-similar, simple wave solution of the Whitham modulation equations, a first order, quasi-linear system of PDEs [34, 4]. Here, the partial DSW modulation is a simple wave solution on the middle characteristics Q in eq. (17) with R_+ and $R_{\bar{u}}$ constant across the entire modulation. The Riemann invariant R_- depends on the self similar variable $R_- = R_-(\xi)$, $\xi = x/t$, and satisfies

$$\lambda_Q(R_{\bar{u}}, R_-(\xi), R_+) = \xi. \quad (19)$$

The constancy of $R_{\bar{u}}$ and R_+ across the modulation implies that their values at the downstream, harmonic wave edge— where $(a, \bar{u}, k) \rightarrow (0, u_+, k_+)$ — are related to their values at the upstream, resonant wavetrain—where $(a, \bar{u}, k) \rightarrow (a_r, u_r, k_r)$ — according to

$$u_+ = u_r - \frac{3}{10}k_r^{-4}a_r^2, \quad (20)$$

$$\frac{24}{\sqrt{30}}u_+ + \frac{5}{\sqrt{30}}k_+^4 = \frac{24}{\sqrt{30}}u_r + \frac{5}{\sqrt{30}}k_r^4 - 2a_r. \quad (21)$$

For any DSW, the speed at the downstream, harmonic edge, s_+ (see Fig. 3), is the group velocity $c_g = \partial_k \omega$

$$s_+ = \lim_{a \rightarrow 0} \lambda_Q = c_{g+} = 6u_+ + 5k_+^4, \quad (22)$$

for the linear dispersion relation $\omega = 6\bar{u}k + k^5$ of the KdV5 equation (cf. (9)). The modulation speed at the upstream, resonant wavetrain edge, s_- (see Fig. 3), is determined by evaluating the middle characteristic speed λ_Q there

$$s_- = \lambda_Q(R_{\bar{u}}, R_-|_{(a, \bar{u}, k) \rightarrow (a_r, u_r, k_r)}, R_+) = 6u_r + 5k_r^4 - \sqrt{30}a_r. \quad (23)$$

In a partial DSW, the modulation speed at the resonant wavetrain edge must equal the phase speed of the resonant wavetrain [9, 50, 51, 52]. Therefore, the nonlinear dispersion relation (9) and eq. (23) imply the additional relation

$$6u_r + 5k_r^4 - \sqrt{30}a_r = 6u_r + k_r^4 - \frac{3}{10} \frac{a_r^2}{k_r^4}. \quad (24)$$

Since u_+ is given, the equations (20), (21), and (24) are three independent relations between the four unknown parameter values a_r , u_r , k_r and k_+ . The final condition is determined by matching the resonant wavetrain to the nonlinear traveling wave structure that provides a transition to the trailing level u_- .

At the trailing edge of the partial DSW, there is a periodic wavetrain—identified as a nonlinearly resonant wavetrain—behind which there is a (negative polarity) solitary wave-like structure which takes the wavetrain to the level u_- behind, as can be seen in Figure 2. The resonant, approximately periodic wavetrain oscillates about the mean level $\bar{u} = \bar{u}_r$. Numerical simulations indicate that the trailing edge is robust and propagates unchanged over long time intervals, which suggests that it is in fact a traveling wave solution of the KdV5 equation (4) in the form $u(x, t) = f(\xi)$, $\xi = x - V_s t$. This traveling wave solution was studied for the Kawahara equation in [35] and links the equilibrium level u_- as $\xi \rightarrow -\infty$

$$\begin{cases} \lim_{\xi \rightarrow -\infty} f(\xi) = u_-, \\ \lim_{\xi \rightarrow -\infty} f'(\xi) = f''(\xi) = f'''(\xi) = f^{(4)}(\xi) = f^{(5)}(\xi) = 0, \end{cases} \quad (25)$$

to a periodic orbit F as $\xi \rightarrow \infty$

$$\begin{cases} \inf_{\varphi_0 \in [0, P)} \lim_{\xi \rightarrow \infty} \|f(\xi) - F(\xi - \varphi_0)\|_\infty = 0, & F(\xi + P) = F(\xi), \\ \frac{1}{P} \int_0^P F(\xi) d\xi = \bar{u}_r. \end{cases} \quad (26)$$

The function F is the nonlinear, periodic, resonant wavetrain, P is the spatial period of the wavetrain and φ_0 is a suitable phase shift that continuously matches the traveling wave to the resonant wavetrain and therefore the partial DSW. The traveling wave, resonant wavetrain, and partial DSW together form an expanding shock-like structure that provides the dynamic transition between the downstream level u_+ and the upstream level u_- . Following [35], we term this a traveling dispersive shock wave or TDSW.

What remains is to determine the additional relation that, along with equations (20), (21) and (24), uniquely determines the four TDSW parameters a_r , u_r , k_r , and k_+ . For this, we continue to utilize the Stokes wave approximation (7) for the traveling wave's periodic orbit $F(\xi)$ with amplitude a_r , mean u_r , and wavenumber k_r . Then the traveling wave's velocity V_s is given by the Stokes wave phase velocity

$$V_s = 6\bar{u}_r + k_r^4 - \frac{3}{10} \frac{a_r^2}{k_r^4}. \quad (27)$$

Seeking a traveling wave solution $u = f(x - V_s t)$ for the KdV5 equation (4) yields

$$-V_s f' + 6f f' + f^{(5)} = 0. \quad (28)$$

Integrating and applying the boundary conditions (25)

$$-V_s f + 3f^2 + f^{(4)} = (3u_- - V_s)u_-. \quad (29)$$

Integrating and applying boundary conditions a second time, we have

$$-\frac{V_s}{2} f^2 + f^3 + f' f''' - \frac{1}{2} (f'')^2 = (3u_- - V_s) f u_- + \frac{u_-^2}{2} (V_s - 4u_-). \quad (30)$$

The traveling wave equations (29) and (30) represent relations for the traveling wave. Our sole interest with this TDSW solution is the dispersion relation for its trailing edge velocity V_s . This can be obtained from the differential equations (29), (30) evaluated at the wave minimum f_{\min} . Hence,

$$-V_s f_{\min} + 3f_{\min}^2 + f_{\min}''' = (3u_- - V_s)u_- \quad (31)$$

and

$$-\frac{V_s}{2} f_{\min}^2 + f_{\min}^3 - \frac{1}{2} (f_{\min}'')^2 = (3 - V_s) f_{\min} u_- + \frac{u_-^2}{2} (V_s - 4u_-). \quad (32)$$

We estimate f_{\min} , f''_{\min} and f''''_{\min} by utilizing the Stokes wave approximation (7)

$$f_{\min} = \bar{u}_r - a_r - \frac{a_r^2}{10k_r^4}, \quad f''_{\min} = a_r k_r^2 + \frac{2}{5} \frac{a_r^2}{k_r^2}, \quad f''''_{\min} = -a_r k_r^4 - \frac{8}{5} a_r^2. \quad (33)$$

The differential equation expression (31) is used in place of the relation between f_{\min} and f''_{\min} which would be known if the traveling wave solution were known exactly. With these approximations, the TDSW—the resonant wavetrain and the partial DSW that brings it down to the level u_+ —is determined by (21), (20), (27), (31) and (32) on using (33).

The system of nonlinear algebraic equations is provided here to make this process explicit

$$V_s = 6\bar{u}_r + k_r^4 - \frac{3}{10} \frac{a_r^2}{k_r^4}, \quad (34)$$

$$u_r = \frac{3}{10} k_r^{-4} a_r^2, \quad (35)$$

$$\frac{5}{\sqrt{30}} k_+^4 = \frac{24}{\sqrt{30}} u_r + \frac{5}{\sqrt{30}} k_r^4 - 2a_r, \quad (36)$$

$$-V_s f_{\min} + 3f_{\min}^2 + f''''_{\min} = (3u_- - V_s)u_- \quad (37)$$

$$-\frac{V_s}{2} f_{\min}^2 + f_{\min}^3 - \frac{1}{2} (f''_{\min})^2 = (3 - V_s) f_{\min} u_- + \frac{u_-^2}{2} (V_s - 4u_-), \quad (38)$$

where f_{\min} and its derivatives are defined in Eq. (33). The system (34)–(38) can be solved for the unknown variables \bar{u}_r , k_r , a_r , k_+ and V_s to determine the TDSW wave properties.

4. TDSW trailing edge: a genuine traveling wave

Rather than match the partial DSW to a resonant wavetrain that is approximated by a Stokes wave as in the previous Section, in this section, we match the partial DSW to a numerically computed traveling wave solution to KdV5 that satisfies the boundary conditions (25) and (26). The traveling wave solutions were obtained using Matlab's `bvp5c` collocation on the ode (29) for the truncated interval $\xi \in [-L, L]$ with

$$f(-L) = u_-, \quad f'(\pm L) = 0 \quad (39)$$

and f satisfying (32) at $\xi = L$, which is assumed to be a minimum of the traveling wave.

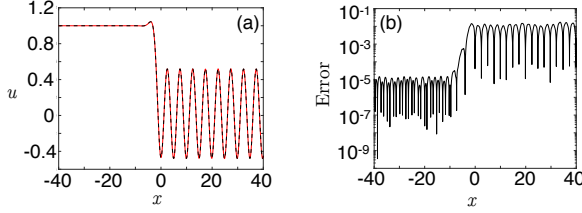


Figure 4. Comparison of the trailing edge of the TDSW numerical solution for the KdV5 (4) with unit step initial data and the boundary value problem from (28). (a) overlay of the two solutions, (b) absolute difference between the two solutions.

An initial guess for the numerical solver is taken from simulations of the initial value problem (3) with unit jump initial data $u_- = 1$ and $u_+ = 0$. To obtain accurate comparisons with time-dependent numerical simulations, the mean of the periodic portion of the traveling wave is set to $\bar{u}_r = 0.0298$, which is estimated from time-dependent numerical simulations. The domain is truncated to only include the traveling wave. The parameters obtained from numerical solutions are

$$V_s = 2.703, \quad a_r = 0.498, \quad k_r = 1.265. \quad (40)$$

Scaling invariants of the KdV5 (4) allows one to deduce that for arbitrary step initial conditions (3), the traveling wave properties become

$$V_s = K_1(u_- - u_+), \quad a_r = K_2(u_- - u_+), \quad k_r = K_3(u_- - u_+)^{1/4}, \quad (41)$$

where K_i , $i = 1, 2, 3$, are numerical constants with $K_1 = 2.703$, $K_2 = 0.498$ and $K_3 = 1.265$. The sole interest now is to determine the matching of the traveling wave with the leading partial DSW via the Riemann invariants R_- and $R_{\bar{u}}$ (given by Eqs. (17) and (16), respectively). To demonstrate the validity of the TDSW trailing edge as a genuine traveling wave, in Figure 4 we have overlaid the numerical solution of the initial value problem (3) for the KdV5 equation (4) on this solution of the boundary value problem, Eq. (28) with boundary conditions (25) and (26). The boundary value problem solution and the

full pde solution only differ by $O(10^{-2})$, verifying that the trailing edge is, in fact, approximately a genuine traveling wave.

The remaining macroscopic TDSW properties can then be determined from the simple wave characteristic conditions (21) and (20), where the leading wavenumber k_+ and periodic wavetrain mean, \bar{u}_r are given in terms of a_r , k_{rmr} and V_s . In terms of the numerical constants K_i , we have

$$k_+^4 = \left(\frac{36}{25} \frac{K_2^2}{K_3^4} + K_3^4 + 2 \frac{\sqrt{30}}{5} K_2 \right) (u_- - u_+) \quad (42)$$

$$\bar{u}_r = \frac{3}{10} \frac{K_2^2}{K_3^4} (u_- - u_+) + u_+, \quad (43)$$

which yield an alternative mechanism to compute the macroscopic wave properties of the TDSW— both the traveling wave upstream edge and partial DSW downstream edge.

5. Comparisons of KdV5 Modulation Theory with Numerical Solutions

In this section, the modulation theory solution of Section 3 for the resonant wavetrain and partial DSW (the TDSW) will be compared with numerical solutions of the KdV5 equation (4). These comparisons are made for the scaled Riemann problem initial conditions (4) with $u_- = 1$ and $u_+ = 0$. Solutions for non-unit jumps for $u_- \neq 1$ or $u_+ \neq 0$ can be obtained by scaling and Galilean transformations. The numerical solutions of the KdV5 equation (4) were obtained by a standard pseudo-spectral Fourier scheme [58, 59, 60] on u_x so that a truncated Fourier series well approximates the initial data. The initial data was taken to be a smooth hyperbolic tangent profile connecting the far-field constant states. The numerical method uses fast Fourier transforms to approximate spatial derivatives and then advances in time using the 4th order Runge-Kutta (RK4) scheme. A typical time step used for simulation $\Delta t = 0.005$ and the spatial domain was chosen to be sufficiently large so that wave interaction with boundaries was negligible.

Figure 5 illustrates comparisons between the modulation theory solution of Section 3 for the TDSW and the numerical solution of the KdV5 equation (4). Figure 5(a) shows a space-time contour plot of the

numerical solution up to $t = 50$. It can be seen that modulation theory gives an accurate estimation of the trailing and leading edge velocities V_s and c_{g+} , respectively. Figure 5(b) depicts a portion of the trailing resonant wavetrain at $t = 50$ from direct numerical simulation and its predicted envelope from the modulation solution's mean height u_r and amplitude a_r . Although the numerical solution develops a small envelope modulation that is not predicted from leading order modulation theory, as the resonant wavetrain approaches the trailing edge, its envelope is well-approximated from modulation theory. The mean height from modulation theory is $\bar{u}_{r,\text{theory}} = 0.0279$, compared with that obtained from the numerical solution $\bar{u}_{r,\text{numerics}} = 0.0298$.

Figure 5(c) shows a portion of the Fourier spectrum of the numerical solution at $t = 50$. The peak due to the resonant wavetrain can be clearly seen and is in excellent agreement with that given by the resonance condition (27).

Finally, Figure 5(d) illustrates the leading edge partial DSW at $t = 50$ and its envelope predicted from modulation theory. The envelope was computed using the simple wave solution (19). This solution expresses the wavenumber k , mean height \bar{u} and amplitude a in terms of the self-similar variable $\xi = x/t$. The Stokes expansion (7) then gives the upper envelope of the modulated wavetrain as $\bar{u}(x/t) + a(x/t) + \alpha_2 a^2(x/t)$ and the lower envelope as $\bar{u}(x/t) - a(x/t) + \alpha_2 a^2(x/t)$, which yields a good approximation to the numerical solution of the KdV5 equation (4). The numerical solution shows no clear, definite linear edge to the partial DSW, with a small amplitude wavetrain propagating ahead of the structure. This is a common feature in DSW theory [4].

6. Linear resonance in the Kawahara Equation

In Section 3, a modulation theory solution was found for the TDSW solution of the KdV5 equation (4). In the presence of weak third order dispersion, the DSW structure arising in the Kawahara equation remains familiar (see, e.g. Fig. 1(c)). Figure 6 presents numerical results for the trailing edge velocity V_s , wavenumber k_r , amplitude a_r and mean height \bar{u}_r of the resonant wave of the TDSW solution of the Kawahara equation (1) as a function of the third order dispersion coefficient ϵ . In the range $0 \leq \epsilon \leq 2$, the DSW remains a TDSW. It can be seen that the trailing edge velocity V_s is quite insensitive to the value of ϵ , with the ampli-

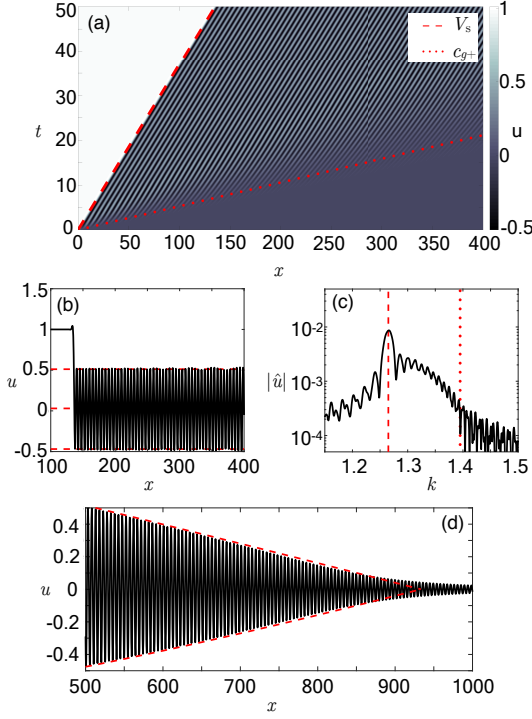


Figure 5. Comparisons of modulation theory solution for the KdV5 equation (4) (dashed) with numerical solutions for unit step initial data (3) $u_+ = 0$ and $u_- = 1$ (solid). (a) Space-time contour plot overlaid with the trailing V_s and leading edge TDSW c_{g+} velocities from modulation theory predictions, (b) trailing edge of the TDSW at $t = 50$ and the resonant wavetrain envelope, (c) the Fourier transform of the numerical solution at $t = 50$ with the resonant wavenumber prediction k_r (dashed) and the wavenumber k_+ (dotted) of the partial DSW leading edge, (d) leading edge of the TDSW at $t = 50$ and the partial DSW envelope.

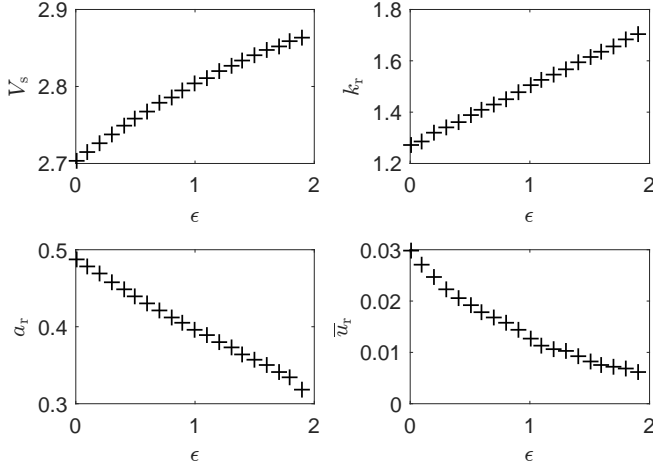


Figure 6. Resonant wave (a) trailing edge velocity V_s , (b) wavenumber k_r , (c) amplitude a_r and (d) mean height \bar{u}_r as a function of the coefficient of the third order dispersion ϵ in the Kawahara equation (1). Here $u_- = 1$ and $u_+ = 0$.

tude a_r moderately sensitive. However, the periodic wave wavenumber k_r and amplitude a_r vary extensively with ϵ , while the mean level \bar{u}_r rapidly vanishes with the third order dispersion coefficient. This is to be expected, since as ϵ increases the Kawahara equation approaches the KdV equation, which does not have a TDSW solution. The amplitude and mean height of the resonant wavetrain must then vanish as ϵ increases. The reason for the more rapid decay of the mean height as compared with the amplitude can be found on developing the weakly nonlinear modulation theory for the Kawahara equation, as was done for the 5th order KdV equation in Section 2. The inclusion of both third and fifth order dispersion complicates the modulation equations, however, and the simplicity of the analysis of the TDSW structure is lost. In this section we will address some of the complications that arise when the DSW is in the intermediate region exhibiting both features of a classical, KdV-like DSW for large ϵ and the nonclassical TDSW for small ϵ .

In this section, we explore the effect of including moderate third order dispersion in the Kawahara equation (1) which has the linear dispersion relation (2) for linear waves on the mean level \bar{u} . The dispersion relation is non-convex ($\omega_{kk} = 0$ at a point), which, in this case, leads to a resonance between linear and nonlinear, e.g. solitary, waves [37, 38, 39]. The situation for a DSW is more complicated in that it consists of a continuous series of modulated nonlinear waves. Hence, in principle, every wave in the DSW could resonate and produce radiation of different wavenumbers. Furthermore, the non-convexity of the dispersion relation (2) breaks a typical assumption of DSW theory [4]. All of this is indicated by the modulation of the DSW and resonant wavetrain ahead of it, as seen in Figure 1(b) [35].

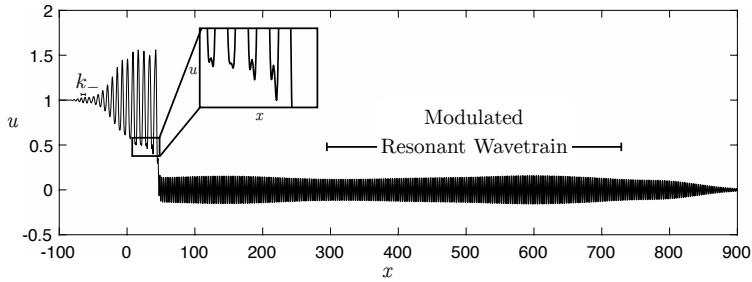


Figure 7. Dispersive shock wave for moderate third order dispersion, $\epsilon = 5$ in the Kawahara equation (1). The leading resonant wavetrain is non-uniformly modulated. The nearly classical DSW at the trailing edge is corrupted by small linear modulations due to the linear internal resonance, shown in the inset.

Without loss of generality, we study the Riemann problem (3) with $u_- = 1$ and $u_+ = 0$ for the Kawahara equation (1) with the parameter $\epsilon > 0$. We begin our analysis by revisiting the dispersive shock fitting method applied to the Kawahara equation [35]. DSW fitting [4, 56, 57] is based on the observation that, for typical Whitham modulation systems, the zero wavenumber and zero amplitude limits of the Whitham modulation equations are degenerate. A consequence of this is that the

linear edge of the DSW can be found through the ODE

$$\frac{dk}{d\bar{u}} = \frac{\frac{\partial \omega}{\partial \bar{u}}}{6\bar{u} - \frac{\partial \omega}{\partial k}}, \quad k(u_+ = 0) = 0, \quad (44)$$

where $\omega(k, \bar{u})$ is the linear dispersion relation. The location of the boundary condition $\bar{u} = u_+ = 0$ assumes negative dispersion, $\omega_{kk}(k_-, u_-) < 0$, at the trailing, harmonic edge, so that the DSW's oscillations remain well-ordered. Using the dispersion relation (2), the solution for the trailing edge wavenumber $k_- = k(u_- = 1)$ is

$$k_-^2 = \frac{3}{5} \left\{ \epsilon - \left[\epsilon^2 - \frac{40}{3} \right]^{1/2} \right\}. \quad (45)$$

Evaluating $\omega_{kk}(k_-, 1)$, we observe that $\omega_{kk}(k_-, 1) < 0$ so long as $\epsilon > 4\sqrt{10}/3 \approx 4.22$.

The leading, solitary wave edge of the DSW is determined by so-called conjugate wavenumber \tilde{k} and frequency $\tilde{\omega}$ that result in the conjugate ODE problem

$$\frac{d\tilde{k}}{d\bar{u}} = \frac{\frac{\partial \tilde{\omega}}{\partial \bar{u}}}{6\bar{u} - \frac{\partial \tilde{\omega}}{\partial \tilde{k}}}, \quad \tilde{k}(u_- = 1) = 0. \quad (46)$$

Here, the conjugate dispersion relation $\tilde{\omega}(\tilde{k}, \bar{u})$ is obtained from the linear dispersion relation (2) upon setting $k \rightarrow i\tilde{k}$ and $\omega \rightarrow -i\tilde{\omega}$:

$$\tilde{\omega} = 6\bar{u}\tilde{k} + \epsilon\tilde{k}^3 + \tilde{k}^5. \quad (47)$$

The precise reasons for this substitution are related to the structure of the Whitham modulation equations for KdV-type equations in the solitary wave limit. As for the trailing, linear edge, this equation can be solved to yield the conjugate wavenumber $\tilde{k}_+ = k(u_+ = 0)$ at the leading, solitary wave edge

$$\tilde{k}_+^2 = \frac{3}{5} \left\{ -\epsilon + \left[\epsilon^2 + \frac{40}{3} \right]^{1/2} \right\}. \quad (48)$$

It can be seen from the solution (45) that the trailing edge wavenumber ceases to be real for $\epsilon^2 < 40/3$, which implies that the DSW is not classical for sufficiently small ϵ . This change in behavior gives a reason for the change from a RDSW to a crossover DSW. Unfortunately, dispersive shock fitting only applies to the edges of a DSW and not

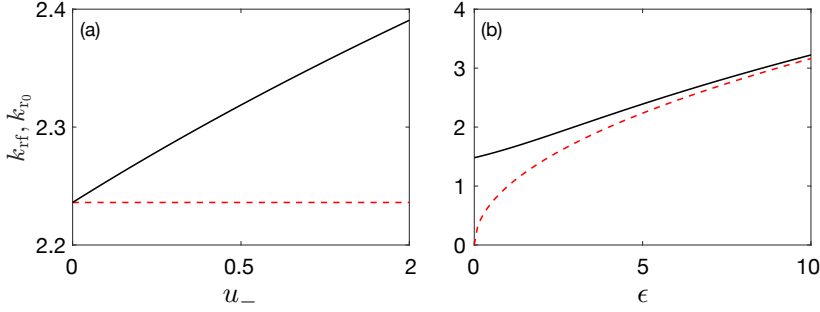


Figure 8. Resonant wavenumbers generated by DSW. Wavenumber k_{rf} generated by lead solitary wave: black (solid) line; wavenumber k_{r0} generated by wave with 0 velocity: red (dashed) line. (a) Resonant wavenumber dependence on jump height for $u_+ = 0$ and $\epsilon = 5$, (b) resonant wavenumber dependence on ϵ for $u_+ = 0$ and $u_- = 1$.

its interior. Without the full Whitham modulation equations for the Kawahara equation (1) the detailed changes in the DSW as it goes from a RDSW to a crossover DSW cannot be analyzed. This change in behavior at the trailing shock edge is backed up by Fig. 7 where it can be seen that the trailing edge of a crossover DSW is truncated as compared with the classical DSW of Figure 1(a).

The wavenumber of the resonant wavetrain generated by the lead solitary wave in the DSW can now be calculated, so long as the resonant wavetrain is linear. As stated above, each wave of the DSW generates its own resonant wavenumber. The wavenumber k_{rf} generated by the lead solitary wave of the DSW is obtained by equating the phase velocity given by (2) with the lead solitary wave velocity $\tilde{\omega}/k_+$, see (47), giving

$$\epsilon \tilde{k}_+^2 + \tilde{k}_+^4 = -\epsilon k_{rf}^2 + k_{rf}^4, \quad (49)$$

so that

$$k_{rf}^2 = \frac{1}{2} \left[\epsilon + \left[\epsilon^2 + 4 \left(\epsilon \tilde{k}_+^2 + \tilde{k}_+^4 \right) \right]^{1/2} \right]. \quad (50)$$

The RDSW and crossover DSW solutions of the Kawahara equation (1) have a leading, solitary wave edge with positive velocity and a trailing, linear wave edge with negative velocity, see Figure 1. Hence, there is a wave in these DSWs which has zero velocity. The resonant wave

generated by this particular DSW component then has 0 velocity, so that from the linear dispersion relation (2) the wavenumber k_{r0} of this particular resonant wave is

$$k_{r0} = \sqrt{\epsilon}. \quad (51)$$

These resonant wavenumbers are illustrated as functions of the rear level u_- and of ϵ in Figure 8. It can be seen that the range of wavenumbers generated through the DSW is small, except in the limit $\epsilon \rightarrow 0^+$ in which the Kawahara equation (1) becomes the KdV5 equation with fifth order dispersion only. The DSW structure for the KdV5 equation is a TDSW only, for which the analysis resulting in the leading, solitary wave edge expression (48) does not apply.

As shown in Figure 8, the range of resonant wavenumbers generated in the DSW for the Kawahara equation (1) is small when the coefficient ϵ of the third order dispersion is not small, $\epsilon > 2$ approximately. The interaction of these resonant waves, a resonant wave packet, leads to the modulations of the resonant wavetrain ahead of the crossover DSW seen in Figure 1(b).

7. Complex Characteristic Speeds for the Kawahara Equation

The modulation theory of Section 2 for the KdV5 equation (4), can be extended to find modulation equations for the Kawahara equation (1) that incorporates third order dispersion. The derivation of these modulation equations from the Stokes wave solution and the Lagrangian for the Kawahara equation is similar to the derivation of Section 2 for the KdV5 equation, so only the basic details will be given here. The third derivative can result in the modulation equations being elliptic, so that the underlying Stokes wave is modulationally unstable [1].

The Kawahara equation (1) has the Lagrangian for the potential ϕ , with $u = \phi_x$,

$$L = \frac{1}{2}\phi_x\phi_t + \phi_x^3 - \frac{1}{2}\epsilon\phi_{xx}^2 + \frac{1}{2}\phi_{xxx}^2. \quad (52)$$

The Kawahara equation also possesses a weakly nonlinear Stokes wave solution

$$u = \bar{u} + a \cos \theta + \frac{a^2}{2k^2(\epsilon - 5k^2)} \cos 2\theta + \dots \quad (53)$$

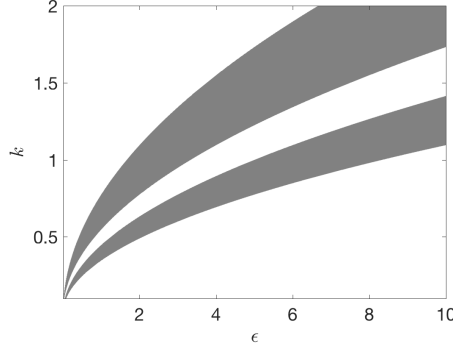


Figure 9. Existence of non-zero imaginary part of characteristic velocities (gray regions) for the Kawahara-Whitham modulation equations (59) with wavenumber k and third order derivative coefficient ϵ .

for small amplitude a , so long as $\epsilon \neq 5k^2$ and $a \ll k^2|\epsilon - 5k^2|$. The phase θ and dispersion relation are

$$\theta = kx - \omega t, \quad \omega = 6\bar{u}k - \epsilon k^3 + k^5 + \frac{3a^2}{2k(\epsilon - 5k^2)}. \quad (54)$$

Substituting this Stokes expansion into the Lagrangian (52) and averaging over the rapid phase θ it is found that the averaged Lagrangian is

$$\mathcal{L} = -\frac{1}{2}\gamma\bar{u} + \bar{u}^3 + \left(\frac{3}{2}\bar{u} - \frac{1}{4}\frac{\omega}{k} - \frac{\epsilon}{4}k^2 + \frac{1}{4}k^4\right)a^2. \quad (55)$$

Taking variations of the averaged Lagrangian (55) with respect to the mean height \bar{u} , amplitude a , phase θ ($k = \theta_x$ and $\omega = -\theta_t$) and the pseudo-phase ψ ($\bar{u} = \psi_x$ and $\gamma = -\psi_t$) results in the modulation equations

$$\frac{\partial \bar{u}}{\partial t} + \frac{\partial}{\partial x} \left(3\bar{u}^2 + \frac{3}{2}a^2 \right) = 0, \quad (56)$$

$$\frac{\partial}{\partial x}(a^2) + \frac{\partial}{\partial x} (6\bar{u}a^2 - 3\epsilon k^2 a^2 + 5a^2 k^4) = 0, \quad (57)$$

$$\frac{\partial k}{\partial t} + \frac{\partial}{\partial x} \left(6\bar{u}k - \epsilon k^3 + k^5 + \frac{3a^2}{2k(\epsilon - 5k^2)} \right) = 0 \quad (58)$$

to second order in the small amplitude a . The first two modulation equations are conservation of mass and momentum, respectively. The last equation (58) is conservation of waves. These modulation equations can be set in the quasi-linear matrix form

$$q_t + \mathcal{A}q_x = 0, \quad (59)$$

where

$$\mathcal{A} = \begin{bmatrix} \bar{u} & \frac{3}{2} & 0 \\ 6a^2 & 6\bar{u} - 3\epsilon k^2 + 5k^4 & -6\epsilon a^2 k + 20k^3 a^2 \\ 6k & \frac{3}{2k(\epsilon - 5k^2)} & 6\bar{u} - 3\epsilon k^2 + 5k^4 + \frac{3a^2(15k^2 - \epsilon)}{2k^2(\epsilon - 5k^2)^2} \end{bmatrix}. \quad (60)$$

Three distinct, real eigenvalues of \mathcal{A} (characteristic velocities) correspond to hyperbolicity of the Whitham equations and modulational stability of the Stokes wave. If any eigenvalues are not purely real, the Stokes wave is modulationally unstable [1]. As a test case, let us consider the nonlinear resonant wavetrain in the TDSW for the KdV5 equation (4) where $\bar{u} \ll 1$, $u_- = 1$, $u_+ = 0$, and $\epsilon = 0$. This case corresponds to the modulation equations of Section 2 for the KdV5 equation for which the modulation equations are hyperbolic. For these values,

$$a \approx 0.49, \quad k \approx 1.26, \quad \bar{u} \approx 0.03. \quad (61)$$

Numerical calculations and eigenvalue expansions show that $\Im \lambda = 0$ in the regime $\epsilon = 0$, which is expected as the modulation equations (56)–(58) then reduce to the fifth order KdV modulation equations (13)–(15). From numerical solutions, it is found that for $\Delta = 1$ the TDSW starts to drastically change form near $\epsilon = 2.6$, which implies there is a nontrivial change in the nonlinear wavetrain as ϵ increases. In order to completely quantify the transition to modulational instability of the TDSW wavetrain we need to compute the eigenvalues of the matrix in the modulation system (59).

To calculate the eigenvalues of the matrix (60), that is the characteristic velocities of the modulation system (59), we re-write the matrix in the form

$$\mathcal{A} = \begin{bmatrix} 6\bar{u} & \frac{3}{2} & 0 \\ 6a^2 & \omega_k & \omega_{kk}a^2 \\ 6k & \beta_1 & \omega_k + a^2\beta_2 \end{bmatrix}, \quad (62)$$

where

$$\beta_1 = \frac{3}{2k(\epsilon - 5k^2)} \quad (63)$$

$$\beta_2 = \frac{3(15k^2 - \epsilon)}{2k^2(\epsilon - 5k^2)^2} = \frac{15k^2 - \epsilon}{2k}\beta_1. \quad (64)$$

It is known that in the zero amplitude limit, two of the characteristic velocities coincide with the linear group velocity and the third is the long wave speed $6\bar{u}$ [1]. In the weakly nonlinear regime $a \ll 1$, the correction to the long wave speed is of order a^2 , whereas the degenerate group velocity ω_k exhibits an order a correction. Therefore, in the weakly nonlinear regime, complex eigenvalues must appear from the nonlinear splitting of ω_k . We seek a perturbation series solution of the form

$$\lambda_{\text{gv}} = \omega_k + a\lambda_1 + \dots \quad (65)$$

It is then found that

$$\lambda \sim \omega_k \pm a \sqrt{15k^2 \left(\frac{6}{5k^2 - 3\epsilon} + \frac{1}{5k^2 - \epsilon} \right) + 9 + o(a)}, \quad (66)$$

which reduce to the characteristic velocities in Eqs. (17) and (18) for $\epsilon = 0$. We first note that for $\epsilon \leq 0$, the characteristic velocities are purely real in the weakly nonlinear regime. Thus, modulationally instability is not expected. The Riemann problem for $\epsilon = -1$ was studied in [35] and shown to give rise to a classical DSW with positive dispersion for sufficiently large jump heights. It would therefore be interesting to study the transition from the non-classical TDSW to the classical DSW when $\epsilon < 0$ in future work.

On the other hand, when $\epsilon > 0$, the characteristic velocities (66) can become non-real, so the Stokes wavetrain is unstable. The gray regions in Figure 9 depict the (k, ϵ) parameter space for which the characteristic velocities are complex. Recent work characterizing modulational instability of small amplitude periodic solutions to subharmonic perturbations has shown that modulational instability occurs in the parameter regimes considered here [61].

When the characteristic velocities are not real, a standard DSW cannot exist. We speculate that this regime corresponds to a so-called crossover DSW [35], exhibiting non-monotonic modulations, as seen in Figure 1(b). Such non-monotonic structures have also been observed in

DSWs for the focusing NLS equation for which the Whitham equations exhibit complex characteristic velocities [62].

8. Conclusions

The nonlinear, resonant wavetrain, or traveling dispersive shock wave (TDSW), generated by a dispersive shock wave (DSW) governed by the fifth order Korteweg-de Vries (KdV5) equation, has been analyzed. The TDSW was analyzed in detail using Whitham modulation theory. Whitham modulation equations for the KdV5 equation (4) were found in the weakly nonlinear limit, the regime that coincides with the small amplitude resonant wavetrain for the TDSW. It was found that the resonant wavetrain for a TDSW consists of a (nearly) constant amplitude wavetrain with a partial DSW that brings it down to the level u_+ ahead. The partial DSW consists of linear dispersive waves at its leading edge, but terminates at a weakly nonlinear periodic wave at its trailing edge, determined by the condition that the modulation characteristic velocity matches the phase velocity of the resonant wave, in contrast to a full DSW which terminates at a solitary wave. The partial DSW is accompanied by a mean level change, so that the resonant wavetrain behind it is raised above the level u_+ . This modulation theory solution consisting of a near-constant amplitude resonant wavetrain preceded by a partial DSW was found to be in good agreement with numerical solutions.

The modulation theory developed in this paper can be extended to describe TDSWs in the presence of sufficiently weak third order dispersion ($\epsilon \neq 0$). While the Whitham modulation theory developed for the full Kawahara equation (1) could be used to derive the full description of the resonant wavetrain and its leading partial DSW, this is complicated by the possible ellipticity of these modulation equations as ϵ increases from 0. The weakly nonlinear modulation equations of Section 7 could benefit from further analysis in order to understand the role of modulational instability in the resonant DSW solution of the Kawahara equation. This question of modulational stability of a resonant DSW and its connection to crossover DSWs is generic and relates to general resonant DSWs and their various forms [4].

References

1. G.B. Whitham, *Linear and Nonlinear Waves*, J. Wiley and Sons, New York (1974).
2. T.B. Benjamin and M.J. Lighthill, "On cnoidal waves and bores," *Proc. Roy. Soc. Lond. A*, **224**, 448–460 (1954).
3. R.S. Johnson, "A non-linear equation incorporating damping and dispersion," *J. Fluid Mech.*, **42**, 49–60 (1970).
4. G.A. El and M.A. Hoefer, "Dispersive shock waves and modulation theory," *Physica D*, **333**, 11–65 (2016).
5. P.G. Baines, "Upstream influence and Long's model in stratified flow," *J. Fluid Mech.*, **82**, 147–159 (1979).
6. P.G. Baines, "Observation of stratified flow over two-dimensional obstacles in fluid of finite depth," *Tellus*, **31**, 351–371 (1979).
7. P.G. Baines, "A unified description of two-layer flow over topography," *J. Fluid Mech.*, **146**, 127–167 (1984).
8. R.H.J. Grimshaw and N.F. Smyth, "Resonant flow of a stratified fluid over topography," *J. Fluid Mech.*, **169**, 429–464 (1986).
9. N.F. Smyth, "Modulation theory solution for resonant flow over topography," *Proc. Roy. Soc. Lond. A*, **409**, 79–97 (1987).
10. D.-B. Huang, G.J. Sibul, W.C. Webster, D.-M. Wu and T.Y. Wu, "Ships moving in the transcritical range," *Proc. Conf. on Behaviour of Ships in Restricted Waters*, Varna, **2**, 26-1–26-10, Varna: Bulgarian Ship Hydrodynamics Centre (1982).
11. D.R. Christie, "Long nonlinear waves in the lower atmosphere," *J. Atmos. Sci.*, **46**, 1462–1491 (1989).
12. R.H. Clarke, R.K. Smith and D.G. Reid, "The morning glory of the Gulf of Carpentaria: an atmospheric undular bore," *Monthly Weather Rev.*, **109**, 1726–1750 (1981).
13. V.A. Porter and N.F. Smyth, "Modelling the morning glory of the Gulf of Carpentaria," *J. Fluid Mech.*, **454**, 1–20 (2002).
14. N.F. Smyth and P.E. Holloway, "Hydraulic jump and undular bore formation on a shelf break," *J. Phys. Ocean.*, **18**, 947–962 (1988).
15. D.R. Scott and D.J. Stevenson, "Magma solitons," *Geophys. Res. Lett.*, **11**, 1161–1164 (1984).
16. D.R. Scott and D.J. Stevenson, "Magma ascent by porous flow," *Geophys. Res. Lett.*, **91**, 9283–9296 (1986).
17. T.R. Marchant and N.F. Smyth, "Approximate solutions for magmon propagation from a reservoir," *IMA J. Appl. Math.*, **70**, 796–813 (2005).
18. N.K. Lowman and M.A. Hoefer, "Dispersive shock waves in viscously deformable media," *J. Fluid Mech.*, **718**, 524–557 (2013).
19. M.D. Maiden, N.K. Lowman, D.V. Anderson, M.E. Schubert and M.A. Hoefer, "Observation of dispersive shock waves, solitons, and their interactions in viscous fluid conduits," *Phys. Rev. Lett.*, **116**, 174501 (2016).
20. W. Wan, S. Jia and J.W. Fleischer, "Dispersive superfluid-like shock waves in nonlinear optics," *Nature Phys.*, **3**, 46–51 (2007).

21. C. Barsi, W. Wan, C. Sun and J.W. Fleischer, "Dispersive shock waves with nonlocal nonlinearity," *Opt. Lett.*, **32**, 2930–2932 (2007).
22. G.A. El, A. Gammal, E.G. Khamis, R.A. Kraenkel and A.M. Kamchatnov, "Theory of optical dispersive shock waves in photorefractive media," *Phys. Rev. A*, **76**, 053183 (2007).
23. W. Wan, D.V. Dylov, C. Barsi and J.W. Fleischer, "Diffraction from an edge on a self-focusing medium," *Opt. Lett.*, **35**, 2819–2821 (2010).
24. J. Fatome, C. Finot, G. Millot, A. Armaroli and S. Trillo, "Observation of optical undular bores in multiple four-wave mixing," *Phys. Rev. X*, **4**, 021022 (2014).
25. G. Xu, M. Conforti, A. Kudlinski, A. Mussot and S. Trillo, "Dispersive dam-break flow of a photon fluid," *Phys. Rev. Lett.*, **118**, 254101 (2017).
26. N. Ghofraniha, C. Conti, G. Ruocco and S. Trillo, "Shocks in nonlocal media," *Phys. Rev. Lett.*, **99**, 043903 (2007).
27. J. Wang, J. Li, Q. Guo and W. Hu, "Observation of surface dispersive shock waves in a self-defocusing medium," *Phys. Rev. A*, **91**, 063819 (2015).
28. T.R. Marchant and N.F. Smyth, "Semi-analytical solutions for dispersive shock waves in colloidal media," *J. Phys. B: Atomic Molec. Opt. Phys.*, **45**, 145401 (2012).
29. X. An, T.R. Marchant and N.F. Smyth, "Optical dispersive shock waves in defocusing colloidal media," *Physica D*, **342**, 45–56 (2017).
30. M.A. Hoefer, M.J. Ablowitz, I. Coddington, E.A. Cornell, P. Engels and V. Schweikhard, "Dispersive and classical shock waves in Bose-Einstein condensates and gas dynamics," *Phys. Rev. A*, **74**, 023623 (2006).
31. B. Meppelink, S. B. Koller, J. M. Vogels, P. van der Straten, E. D. van Ooijen, N. R. Heckenberg, H. Rubinsztein-Dunlop, S. A. Haine and M. J. Davis, "Observation of shock waves in a large Bose-Einstein condensate," *Phys. Rev. A*, **80**, 043606 (2009).
32. P.A.P. Janantha, P. Sprenger, M.A. Hoefer and M. Wu, "Observation of self-cavitating envelope dispersive shock waves in yttrium iron garnet thin films," *Phys. Rev. Lett.*, **119**, 024101 (2017).
33. G.A. El, M.A. Hoefer and M. Shearer, "Dispersive and diffusive-dispersive shock waves for nonconvex conservation laws," *SIAM Rev.*, **59**, 3–61 (2017).
34. A.V. Gurevich and L.P. Pitaevskii, "Nonstationary structure of a collisionless shock wave," *Sov. Phys. JETP*, **38**, 291–297 (1974).
35. P. Sprenger and M.A. Hoefer, "Shock waves in dispersive hydrodynamics with nonconvex dispersion," *SIAM J. Appl. Math.*, **77**, 26–50 (2017).
36. T. Kawahara, "Oscillatory solitary waves in dispersive media," *J. Phys. Soc. Jpn.*, **33**, 260–264 (1972).
37. R. Grimshaw, B. Malomed and E.S. Benilov, "Solitary waves with damped oscillatory tails: an analysis of the fifth-order Korteweg-de Vries equation," *Physica D*, **77**, 473–485 (1994).
38. V.I. Karpman, "Radiation by weakly nonlinear shallow-water solitons due to higher-order dispersion," *Phys. Rev. E*, **58**, 5070–5080 (1998).
39. Y. Tan, J. Yang and D.E. Pelinovsky, "Semi-stability of embedded solitons in the general fifth-order KdV equation," *Wave Motion*, **36**, 241–255 (2002).

40. M. Conforti, F. Baronio and S. Trillo, "Resonant radiation shed by dispersive shock waves," *Phys. Rev. A*, **89**, 013807 (2014).
41. M. Conforti and S. Trillo, "Dispersive wave emission from wave breaking," *Opt. Lett.*, **38**, 3815–3818 (2013).
42. M. Conforti, S. Trillo, A. Mussot and A. Kudlinski, "Parametric excitation of multiple resonant radiations from localized wavepackets," *Sci. Rep.*, **5**, 1–5 (2015).
43. S. Malaguti, M. Conforti and S. Trillo, "Dispersive radiation induced by shock waves in passive resonators," *Opt. Lett.*, **39**, 5626–5629 (2014).
44. N.F. Smyth, "Dispersive shock waves in nematic liquid crystals," *Physica D*, **333**, 301–309 (2015).
45. G. El and N.F. Smyth, "Radiating dispersive shock waves in non-local optical media," *Proc. Roy. Soc. Lond. A*, **472**, 20150633 (2016).
46. P. Guyenne and E. I. Pârau, "Finite-depth effects on solitary waves in a floating ice sheet," *J. Fluid Struct.*, **49**, 242–262 (2014).
47. D.J. Ratliff, "Phase dynamics of periodic wavetrains leading to the 5th order KP equation," *Physica D*, **353–354**, 11–19 (2017).
48. G.B. Whitham, "A general approach to linear and non-linear dispersive waves using a Lagrangian," *J. Fluid Mech.*, **22**, 273–283 (1965).
49. G.B. Whitham, "Non-linear dispersive waves," *Proc. Roy. Soc. London A*, **283**, 238–261 (1965).
50. T.R. Marchant and N.F. Smyth, "Initial-boundary value problems for the Korteweg-de Vries equation", *IMA J. Appl. Math.*, **47**, 247–264 (1991).
51. T.R. Marchant and N.F. Smyth, "The initial-boundary problem for the Korteweg-de Vries equation on the negative quarter-plane," *Proc. Roy. Soc. Lond. A*, **458**, 857–871 (2002).
52. M. A. Hoefer, M. J. Ablowitz and P. Engels, "Piston dispersive shock wave problem," *Phys. Rev. Lett.*, **100**, 084504 (2008).
53. G. A. El, V. V. Geogjaev, A. V. Gurevich, and A. L. Krylov, "Decay of an initial discontinuity in the defocusing NLS hydrodynamics," *Physica D*, **87**, 186–192 (1995).
54. S. Benzoni-Gavage, P. Noble and L. M. Rodrigues, "Slow modulations of periodic waves in Hamiltonian PDEs, with application to capillary fluids," *J. Non. Sci.*, **24**, 711–768 (2014).
55. H. Flaschka, M.G. Forest and D.W. McLaughlin, "Multiphase averaging and the inverse spectral solution of the Korteweg-de Vries equation," *Comm. Pure Appl. Math.*, **33**, 739–784 (1980).
56. G.A. El, V.V. Khodorovskii and A.V. Tyurina, "Determination of boundaries of unsteady oscillatory zone in asymptotic solutions of non-integrable dispersive wave equations," *Phys. Lett. A*, **318**, 526–536 (2003).
57. G.A. El, "Resolution of a shock in hyperbolic systems modified by weak dispersion," *Chaos*, **15**, 037103 (2005).
58. B. Fornberg and G.B. Whitham, "Numerical and theoretical study of certain non-linear wave phenomena," *Phil. Trans. Roy. Soc. Lond. Ser. A*, **289**, 373–404 (1978).

59. T.F. Chan and T. Kerkhoven, “Fourier methods with extended stability intervals for KdV,” *SIAM J. Numer. Anal.*, **22**, 441–454 (1985).
60. L.N. Trefethen, *Spectral Methods in MATLAB*, SIAM, Philadelphia (2000).
61. O. Trichtchenko, B. Deconinck and R. Kollar, “Stability of periodic travelling wave solutions to the Kawahara equation,” arXiv preprint arXiv:1806.08445 (2018).
62. G.A. El, E.G. Khamis and A. Tovbis, “Dam break problem for the focusing non-linear Schrödinger equation and the generation of rogue waves,” *Nonlinearity*, **29**, 2798–2836 (2016).
63. A.M. Kamchatnov, 2015, “Whitham theory for perturbed Korteweg-de Vries equation,” *Physica D*, **333**, 99–106 (2016).

PROGRAM@EPSTOPDF¹ DEPARTMENT OF APPLIED MATHEMATICS, UNIVERSITY OF
COLORADO BOULDER, BOULDER, COLORADO, U.S.A. 80309

PROGRAM@EPSTOPDF² SCHOOL OF MATHEMATICS, UNIVERSITY OF EDINBURGH, THE
KING’S BUILDINGS, PETER GUTHRIE TAIT ROAD, EDINBURGH, SCOTLAND, U.K.,
EH9 3FD